



## Optically Induced Rotation of an Exciton Spin in a Semiconductor Quantum Dot

E. Poem, O. Kenneth, Y. Kodriano, Y. Benny, S. Khatsevich, J. E. Avron, and D. Gershoni

*Department of Physics, The Technion—Israel Institute of Technology, Haifa, 32000, Israel*

(Received 15 February 2011; published 18 August 2011)

We demonstrate control over the spin state of a semiconductor quantum dot exciton using a polarized picosecond laser pulse slightly detuned from a biexciton resonance. The control pulse follows an earlier pulse, which generates an exciton and initializes its spin state as a coherent superposition of its two nondegenerate eigenstates. The control pulse preferentially couples one component of the exciton state to the biexciton state, thereby rotating the exciton's spin direction. We detect the rotation by measuring the polarization of the exciton spectral line as a function of the time difference between the two pulses. We show experimentally and theoretically how the angle of rotation depends on the detuning of the second pulse from the biexciton resonance.

DOI: 10.1103/PhysRevLett.107.087401

PACS numbers: 78.67.Hc, 03.67.Lx, 42.25.Ja, 42.50.Dv

Coherent manipulation of the quantum states of a physical system is a critical step towards novel applications in quantum information processing (QIP). Semiconductor quantum dots (QDs) exhibit atomiclike energy spectrum and are compatible with modern micro- and optoelectronics. They are considered as excellent candidates for forming the building blocks for these future technologies [1], and they form the best interface between quantum light and matter [2–4]. Physical realizations of quantum bits (qubits) and logic gates require controlled two-level systems. The spins of QD-confined charge carriers have been proposed for this task [1,5], and recent experiments successfully demonstrated their state preparation and control. Preparation was achieved either by electron-hole pair photogeneration followed by electrical field induced separation [6–8] or by optical pumping [9–11]. Control of the initiated state was then demonstrated either by the ac-Stark effect, induced by an optical pulse [11,12], or by the accumulation of a geometric phase [13–15]. These impressive achievements require a series of optical pulses and the presence of a strong fixed magnetic field.

A QD-confined electron-hole pair (exciton) is the fundamental optical excitation in QDs, essential for interfacing light qubits with matter spin qubits. It was also proposed for QIP realizations [16,17]. The spin state of the optically active (bright) exciton [18–21] and that of the dark exciton [22] have been directly accessed optically. Moreover, we have recently shown that unlike carriers' spin, the exciton spin can be initiated at any desired state by a single optical pulse [23]. Partial control of the exciton's spin was recently demonstrated [24], albeit the time required for a single operation was comparable to the exciton's radiative lifetime ( $\sim 1$  ns).

Here we demonstrate, for the first time, control over the spin of the bright exciton using a single, few picosecond long, laser pulse. The pulse duration, which is 2 orders of magnitude shorter than the exciton lifetime, permits many coherent operations. Moreover, the same control can be

applied to the spin of the dark exciton, whose lifetime is 3 orders of magnitude longer [25].

Here, we demonstrate this control using a circularly polarized laser pulse, slightly detuned from a resonance of an excited biexciton state. The pulse selectively couples one of the exciton spin states to the biexciton, while leaving the other state unaffected. The method is conceptually similar to that used recently on ensembles of charged QDs [13,14]. The experiment is conducted as follows. At first, a right ( $R$ ) or left ( $L$ ) circularly polarized laser pulse tuned into an excitonic resonance of a single semiconductor quantum dot generates an excited bright exciton. The spin state of this excited exciton has a total angular momentum projection of  $J_z = 1$  ( $|R\rangle$ ) or  $-1$  ( $|L\rangle$ ), respectively. The excited exciton then nonradiatively relaxes to the ground state. As discussed below, the spin is preserved during this fast relaxation [23]. This results in the formation of a coherent superposition of the two nondegenerate ground exciton eigenstates [26,27],

$$|H\rangle = \frac{1}{\sqrt{2}}(|R\rangle + |L\rangle), \quad |V\rangle = \frac{1}{i\sqrt{2}}(|R\rangle - |L\rangle), \quad (1)$$

which by themselves correspond to excitations by horizontally ( $H$ ) or vertically ( $V$ ) linearly polarized pulses, respectively [23]. Since the eigenstates are nondegenerate, they evolve at different paces, and the exciton spin precesses in time between the  $|R\rangle$  and the  $|L\rangle$  states [18–20,23] [Fig. 1(a)]. Resonant excitation by an  $R$ -polarized pulse results in the following spin state precession:

$$\begin{aligned} \psi_i(t) &= \frac{1}{\sqrt{2}}(e^{i\Delta \cdot t}|H\rangle + i|V\rangle) = a|L\rangle + b|R\rangle, \\ a &= ie^{i\Delta \cdot t/2} \sin(\Delta \cdot t/2), \quad b = e^{i\Delta \cdot t/2} \cos(\Delta \cdot t/2), \end{aligned} \quad (2)$$

where  $\hbar\Delta$  is the energy difference between the exciton eigenstates. Then, a second, delayed, circularly polarized pulse is tuned into (or slightly detuned from) an excited biexciton resonance. As illustrated in Fig. 1(b), this

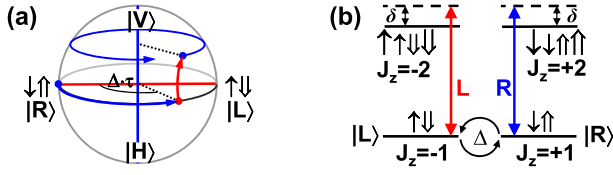


FIG. 1 (color online). (a) A Bloch sphere representation of the exciton spin state. The circle along (above) the equator describes the precession of an exciton spin initialized at  $t = 0$  by an  $R$ -polarized pulse, for  $t < \tau$  ( $t > \tau$ ), where at  $t = \tau$  an  $R$ -polarized biexciton pulse is applied. (b) Schematic description of the relevant exciton and biexciton energy levels and the polarization selection rules for the coupling laser field. The symbol  $\uparrow$  ( $\downarrow$ ) represents an electron (heavy hole) with  $z$ -direction spin projection  $\frac{1}{2}$  ( $-\frac{3}{2}$ ). Short (long) symbols represent charge carriers in their ground (first excited) state.

particular resonant level includes two states, in which the two electron spins are parallel to each other and they are antiparallel to the two holes' spins. The total angular momentum projection of these two states is  $J_z = \pm 2$ . We note that the biexciton resonance used here, where both the electrons and the holes are in triplet configurations, is different than that used in Ref. [23], where the electrons are in a singlet configuration.

Since an  $R$ - ( $L$ -)polarized pulse carries with it angular momentum of 1 ( $-1$ ), when tuned into the biexciton resonance, it couples only the  $J_z = 1$  ( $-1$ ) exciton state to the  $J_z = 2$  ( $-2$ ) biexciton state. The duration of the laser pulse is much shorter than the period of the exciton's precession. Hence, during the pulse, the coupled exciton-biexciton states can be safely viewed as an isolated two-level system [5]. There is an analytical solution for the dynamics of this system for the case of hyperbolic-secant pulse shape [5,28,29]. The coupling that such a pulse induces between the relevant exciton and biexciton states is given by [29]  $C(t) = -\hbar\Omega \operatorname{sech}(\sigma t)e^{-i\omega t}$ , where  $\omega$  is the laser frequency,  $\sigma$  is the pulse bandwidth, and  $\Omega$  is the Rabi frequency. If the exciton spin state just before the second pulse is given by Eq. (2), the state after an  $R$ -polarized hyperbolic-secant pulse is given by [5,29]

$$\begin{aligned} \psi_f = & a|L\rangle + bF(\alpha, -\alpha, \gamma, 1)|R\rangle \\ & + b\frac{i\alpha}{\gamma}F(\alpha + \gamma, -\alpha + \gamma, 1 + \gamma, 1)|J_z = 2\rangle, \end{aligned} \quad (3)$$

where  $F$  is the Gaussian hypergeometric function (also denoted as  ${}_2F_1$ ), and  $\alpha = \frac{\Omega}{\sigma}$ ,  $\gamma = \frac{1}{2} - \frac{i\delta}{2\sigma}$ , where  $\delta = \omega - \omega_0$  is the detuning from the resonance frequency  $\omega_0$ . Using known properties of hypergeometric functions [29], the probability to populate the biexciton if the time difference between the two pulses is  $\tau$ , reads:

$$\begin{aligned} P_{XX} = & |\langle J_z = 2 | \psi_f \rangle|^2 = P_{XX}^0 |b(\tau)|^2 \\ = & \operatorname{sech}^2\left(\frac{\pi\delta}{2\sigma}\right) \sin^2\left(\frac{\pi\Omega}{\sigma}\right) \left[ \frac{1}{2} + \frac{1}{2} \cos(\Delta \cdot \tau) \right]. \end{aligned} \quad (4)$$

A second, nondetuned ( $\delta/\sigma = 0$ )  $\pi$  pulse ( $\Omega/\sigma = 0.5$ ), coincident in time with the first pulse ( $\tau = 0$ ) transfers the entire excitonic population to the biexciton state [5]. In general, the absorption of the second pulse depends on the direction of the precessing exciton spin relative to the polarization of the light pulse [23]. Since the intensity of the photoluminescence (PL) emission from the biexciton spectral lines is a measurement of the pulse absorption, the emission intensity oscillates as the delay between the two pulses increases. These oscillations provide an experimental way to measure the excitonic spin by projecting it onto directions determined by the polarization of the second pulse [23]. The second pulse affects also the nontransferred excitonic population. This is because a circularly polarized pulse couples only one component of the exciton spin state. Thus, the pulse affects the relative amplitude and phase between the excitonic spin eigenstates. The change in relative phase can be interpreted as a "rotation" of the exciton Bloch sphere about the  $|R\rangle$ - $|L\rangle$  axis, and the change in the relative amplitude as "squashing" of the Bloch sphere from the  $|L\rangle$  pole towards the  $|R\rangle$  pole. The exciton state after such an operation is generally expressed, up to normalization, by the first two terms on the right-hand side of Eq. (3). In order to detect it, one needs to measure the spin direction of the exciton after the second pulse. We show below that the excitonic spin projection on the  $|H\rangle$ - $|V\rangle$  axis of the spin Bloch sphere is readily available by measuring the net polarization of the PL from the exciton lines.

The idea is schematically described in Fig. 1(a). As long as the exciton's spin is oriented along the Bloch sphere's equator, its projection on the  $|H\rangle$ - $|V\rangle$  axis is zero, and both eigenstates of the exciton are equally populated. In contrast, if the spin is forced, by the second pulse, to move in a trajectory which leaves the equator, then the populations of the two eigenstates are no longer equal. Once the second pulse is turned off, the exciton spin again precesses around the  $|H\rangle$ - $|V\rangle$  eigenstates axis, and the eigenstate's population difference created during the pulse is kept constant. Since the PL emission is proportional to the probability of population, variations in the population result in measurable changes in the PL from the exciton's spectral lines. Clearly, the normalized difference between the emission intensities of the two cross-linearly polarized exciton lines is a direct experimental measurement of the spin projection on the  $|H\rangle$ - $|V\rangle$  axis of the Bloch sphere. The energy difference between the cross-linearly polarized components is larger than their spectral widths. Therefore, their intensities can be simultaneously measured using a circular polarizer in front of the monochromator.

The excitonic PL emission in our experiment is not temporally resolved. Therefore, it also contains contribution from the biexciton population [Eq. (4)], which decays *incoherently* into excitonic population. However, due to the polarization selection rules [Fig. 1(b)], these incoherent

excitons equally populate the  $|H\rangle$  or  $|V\rangle$  eigenstates, and therefore do not contribute to the eigenstates population difference. The difference can thus be calculated directly from the exciton state immediately after the second pulse, Eq. (3). With Eq. (2) and using properties of hypergeometric functions [29], one obtains

$$\begin{aligned} D_{VH} &= |\langle V|\psi_f\rangle|^2 - |\langle H|\psi_f\rangle|^2 \\ &= -2 \operatorname{Re}[a(\tau)b(\tau)^* F(\alpha, -\alpha, \gamma, 1)^*] \\ &= D_{VH}^0 \sin(\Delta \cdot \tau), \end{aligned} \quad (5)$$

$$\begin{aligned} D_{VH}^0 &= \operatorname{Im} \left[ \frac{\Gamma^2(1/2 + i\delta/2\sigma)}{\Gamma(1/2 + i\delta/2\sigma + \Omega/\sigma)\Gamma(1/2 + i\delta/2\sigma - \Omega/\sigma)} \right], \end{aligned} \quad (6)$$

$\Gamma(z)$  being the Gamma function. Equation (5) shows that the oscillations in  $D_{VH}$  have the same frequency as those of the biexcitonic population, Eq. (4), but they are shifted in phase by  $\pi/2$ . The amplitude of the oscillations, Eq. (6), depends on the pulse intensity ( $\Omega$ ), its bandwidth ( $\sigma$ ), and its detuning ( $\delta$ ). In particular, the sign of the amplitude is given by the sign of the detuning, and on resonance the amplitude vanishes. By using Eqs. (3)–(6), the angle of the induced rotation is given by

$$\theta = \sin^{-1}(D_{VH}^0/\sqrt{1 - P_{XX}^0}). \quad (7)$$

A larger-than- $\pi$  pulse permits any rotation angle.

The studied sample contains one layer of strain-induced InGaAs QDs embedded in the center of a one optical wavelength (in matter) microcavity that enhances the PL collection efficiency. For the optical measurements the sample was placed inside a tube immersed in liquid helium, maintaining sample temperature of 4.2 K. A spatially isolated single QD from a low-density area of the sample was excited with two dye lasers, synchronously pumped by a frequency doubled Nd:YVO<sub>4</sub> passively mode-locked pulsed laser. The dye laser's pulse temporal FWHM was measured to be 9 ps. An *in situ* microscope objective was used both to focus the exciting beams onto the sample and to collect the light emitted from it. The collected light was projected upon a desired polarization, dispersed by a 1 m monochromator, and then detected by either an electrically cooled charge-coupled-device array detector or by a single channel, single photon, silicon avalanche photodetector. The system provides spectral resolution of about 10  $\mu\text{eV}$ . One dye laser was tuned to an excited exciton resonance, 29 meV above the ground-state exciton emission line. Excitation in this resonance results in a high (> 90%) degree of linear polarization memory of the exciton emission line. Moreover, the width of this resonance, which is greater than 500  $\mu\text{eV}$ , is much larger than its polarization splitting of 60  $\mu\text{eV}$  [23]. Therefore,

relaxation to the ground exciton state occurs before any appreciable dephasing or rotation of the spin state can occur, and the spin state of the excited exciton, determined by the polarization of the exciting laser, is preserved during this fast relaxation [22,23]. The other dye laser was tuned into (or slightly detuned from) an excited biexciton resonance, at 33.7 meV above the exciton doublet. Using detailed polarization sensitive spectroscopic studies [30] and a many-carrier theoretical model [31], we unambiguously identified this resonance as the  $J_z = \pm 2$  biexciton states described in Fig. 1(b).

In Fig. 2 we present the  $R$ -polarized PL intensity from the QD versus the PL energy and the time difference ( $\tau$ ) between the first pulse, tuned into the exciton resonance, and the second one, detuned by  $-63 \mu\text{eV}$  from the biexciton resonance. Both lasers were  $R$  polarized. The higher (lower) energy doublet is the emission from the ground-state exciton (biexciton). The oscillations of the PL from the biexciton reflect the precession of the exciton spin state, as initialized by the first pulse [23]. This behavior is described by Eq. (4). The oscillations of the PL from the two excitonic components reflect the variations of the exciton spin projection on the eigenstate's axis, induced by the detuned second pulse, as described by Eq. (5). The line at 1.282 93 eV is due to the positively charged exciton. Its PL does not oscillate with  $\tau$ .

Figure 3(a) presents a PL-excitation spectrum of the biexciton line, for 30 ps difference between the first and second pulse. The intensity of the second pulse was tuned slightly below population inversion at resonance excitation. At this particular intensity the emission intensity from both the exciton and biexciton lines is optimized. This allows simultaneous testing of Eqs. (4) and (5). The dashed line represents the calculated biexciton population [Eq. (4)], for a 9 ps FWHM hyperbolic-secant pulse ( $\hbar\sigma = 145 \mu\text{eV}$ ). The deviation of the measured intensity from

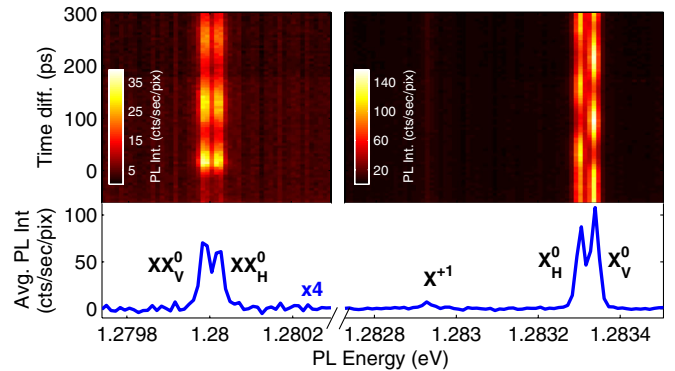


FIG. 2 (color online).  $R$ -polarized PL intensity as a function of the photon energy and the time difference between two  $R$ -polarized laser pulses. The first is tuned into the exciton resonance and the second is detuned by  $-63 \mu\text{eV}$  from the biexciton resonance. The temporally averaged spectrum is shown at the bottom.

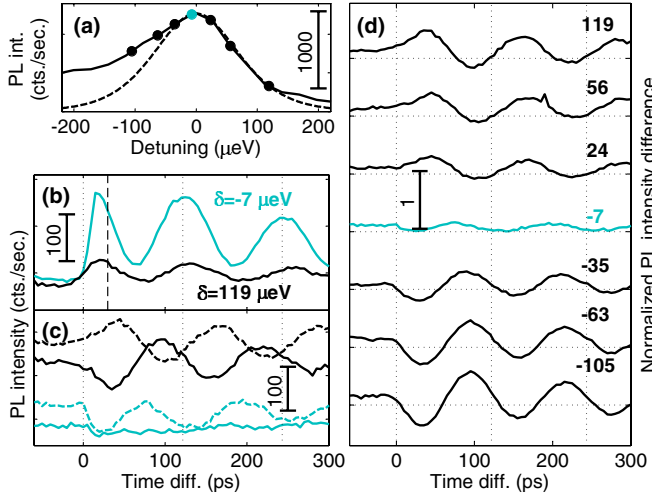


FIG. 3 (color online). (a) Solid line—measured biexciton PL intensity versus the second pulse detuning, at  $\tau = 30$  ps. The circles represent the specific energies used for the measurements presented in (b)–(d). The dashed line is the calculated  $P_{XX}$  [Eq. (4)], for a pulse of 9 ps FWHM ( $\hbar\sigma = 145 \mu\text{eV}$ ). (b) Biexciton intensity versus  $\tau$  close to [gray (light blue)] and far from (black) resonance. The vertical dashed line denotes  $\tau = 30$  ps. (c) Solid (dashed) line denotes PL intensity of the H (V) component of the exciton doublet versus  $\tau$ , close to and far from resonance, as in (b). The curves are vertically shifted for clarity. (d) The differences between the PL from the V and H components, normalized by their sum at negative  $\tau$ , for the energies marked by circles in (a) and specified in  $\mu\text{eV}$  next to each curve. Vertical dotted lines present integer spin precession periods  $T = \hbar/(34 \mu\text{eV}) = 122$  ps.

the theoretical line at low energies is due to a nearby  $J_z = 0$  excited biexciton resonance [30]. We note that the width of the  $J_z = \pm 2$  biexciton resonance is completely determined by the spectral width of the laser. This indicates that any dephasing and relaxation processes are significantly slower than the pulse duration. Indeed, in cw excitation the spectral width of this resonance is significantly narrower. This implies that the  $J_z = \pm 2$  biexciton remains coherent during the second pulse. In Fig. 3(b) we present the intensity of the PL from the biexciton lines as a function of  $\tau$ . The black [gray (blue)] line presents off (almost on) biexcitonic resonant excitation. In both cases, the evolution is cosinusoidal, as in Eq. (4). In Fig. 3(c) we present the intensity of the PL from the exciton lines as a function of  $\tau$ , for both off and almost on resonant excitation as in 3(b). The solid (dashed) line denotes the PL from the H- (V-)polarized component of the excitonic doublet. In Fig. 3(d) we present the difference between the PL intensities from these two cross-linearly polarized components, normalized by their sum at negative delay time (before the second pulse). The oscillations are sinusoidal in time, as in Eq. (5). Their amplitude depends on the detuning from resonance, below (above) resonance, the amplitude is negative (positive) and on resonance it

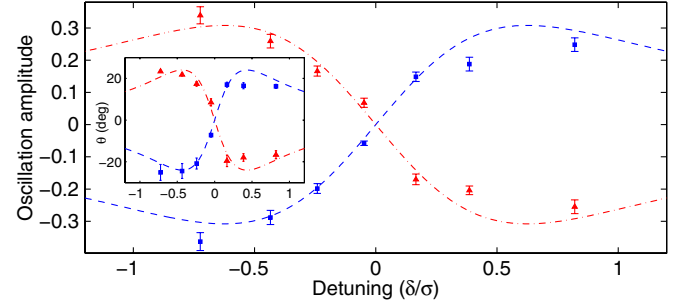


FIG. 4 (color online). Measured (symbols) and calculated (lines) oscillation amplitudes of the exciton polarization versus the detuning  $\delta/\sigma$ , where  $\hbar\sigma = 145 \mu\text{eV}$  and  $\Omega/\sigma = 0.35$  ( $0.7\pi$  pulse). Dark gray (blue) [light gray (red)] color describes co- [cross-]circularly polarized pulses. Inset: The rotation angles  $\theta$  versus the detuning for a  $0.7\pi$  pulse.

vanishes, as expected from Eq. (6). This dependence is summarized in Fig. 4, which presents the amplitudes of the measured oscillations in the exciton polarization versus the normalized detuning,  $\delta/\sigma$ . The lines present the amplitude calculated by Eq. (6), for  $\Omega/\sigma = 0.35$  ( $0.7 - \pi$  pulse), slightly below inversion. The figure describes co- [dark gray (blue)] and cross-circularly [light gray (red)] polarized laser pulses. The measured and calculated spin rotation angles [Eq. (7)] versus the detuning are presented in the inset of Fig. 4. The agreement between the measured rotations and the theoretically calculated ones (which assume no dephasing) indicates a close to unity rotation fidelity.

In summary, we demonstrated that the polarization of the QD exciton spin can be rotated by a single, short optical pulse. We showed that the rotation can be directly detected by monitoring the intensities of the two components of the excitonic spectral line.

The support of the U.S.-Israel Binational Science Foundation (BSF), the Israeli Science Foundation (ISF), the Ministry of Science and Technology (MOST), and that of the Technion's RBNI are gratefully acknowledged.

- 
- [1] D. Loss and D.P. DiVincenzo, *Phys. Rev. A* **57**, 120 (1998).
  - [2] X. Li *et al.*, *Science* **301**, 809 (2003).
  - [3] A. Zrenner *et al.*, *Nature (London)* **418**, 612 (2002).
  - [4] C. Simon *et al.*, *Eur. Phys. J. D* **58**, 1 (2010).
  - [5] S.E. Economou *et al.*, *Phys. Rev. B* **74**, 205415 (2006).
  - [6] M. Kroutvar *et al.*, *Nature (London)* **432**, 81 (2004).
  - [7] R.J. Young *et al.*, *New J. Phys.* **9**, 365 (2007).
  - [8] A.J. Ramsay *et al.*, *Phys. Rev. Lett.* **100**, 197401 (2008).
  - [9] M. Atatüre *et al.*, *Science* **312**, 551 (2006).
  - [10] B.D. Gerardot *et al.*, *Nature (London)* **451**, 441 (2008).
  - [11] D. Press *et al.*, *Nature (London)* **456**, 218 (2008).
  - [12] J. Berezovsky *et al.*, *Science* **320**, 349 (2008).
  - [13] Y. Wu *et al.*, *Phys. Rev. Lett.* **99**, 097402 (2007).
  - [14] A. Greilich *et al.*, *Nature Phys.* **5**, 262 (2009).

- [15] E. D. Kim *et al.*, *Phys. Rev. Lett.* **104**, 167401 (2010).  
[16] F. Troiani, U. Hohenester, and E. Molinari, *Phys. Rev. B* **62**, R2263 (2000).  
[17] E. Biolatti *et al.*, *Phys. Rev. Lett.* **85**, 5647 (2000).  
[18] N. H. Bonadeo *et al.*, *Science* **282**, 1473 (1998).  
[19] T. Flissikowski *et al.*, *Phys. Rev. Lett.* **86**, 3172 (2001).  
[20] S. J. Boyle *et al.*, *Phys. Rev. B* **78**, 75301 (2008).  
[21] H. Kosaka *et al.*, *Phys. Rev. Lett.* **100**, 096602 (2008).  
[22] E. Poem *et al.*, *Phys. Rev. B* **81**, 085306 (2010).  
[23] Y. Benny *et al.*, *Phys. Rev. Lett.* **106**, 040504 (2011).  
[24] A. Boyer de la Giroday *et al.*, *Phys. Rev. B* **82**, 241301 (2010).  
[25] J. McFarlane *et al.*, *Appl. Phys. Lett.* **94**, 093113 (2009).  
[26] D. Gammon *et al.*, *Phys. Rev. Lett.* **76**, 3005 (1996).  
[27] V. D. Kulakovskii *et al.*, *Phys. Rev. Lett.* **82**, 1780 (1999).  
[28] N. Rosen and C. Zener, *Phys. Rev.* **40**, 502 (1932).  
[29] T. Takagahara, *J. Opt. Soc. Am. B* **27**, A46 (2010).  
[30] Y. Benny *et al.*, arXiv:1105.4861v1.  
[31] E. Poem *et al.*, *Phys. Rev. B* **76**, 235304 (2007).